GEOLOGY | THE GEOLOGICAL SOCIETY OF AMERICA®

https://doi.org/10.1130/G45793.1

Manuscript received 8 November 2018
Revised manuscript received 18 January 2019
Manuscript accepted 20 February 2019

Published online 11 March 2019

Boundary condition controls on the high-sand-flux regions of Mars

Matthew Chojnacki[1], Maria E. Banks[2], Lori K. Fenton[3], and Anna C. Urso[1]
[1]Lunar and Planetary Laboratory, University of Arizona, Tucson, Arizona 85721, USA
[2]National Aeronautics and Space Administration (NASA) Goddard Space Flight Center, Greenbelt, Maryland 20771, USA
[3]Carl Sagan Center at the SETI (Search for Extra-Terrestrial Intelligence) Institute, Mountain View, California 94043, USA

ABSTRACT

Wind has been an enduring geologic agent throughout the history of Mars, but it is often unclear where and why sediment is mobile in the current epoch. We investigated whether eolian bed-form (dune and ripple) transport rates are depressed or enhanced in some areas by local or regional boundary conditions (e.g., topography, sand supply/availability). Bed-form heights, migration rates, and sand fluxes all span two to three orders of magnitude across Mars, but we found that areas with the highest sand fluxes are concentrated in three regions: Syrtis Major, Hellespontus Montes, and the north polar erg. All regions are located near prominent transition zones of topography (e.g., basins, polar caps) and thermophysical properties (e.g., albedo variations); these are not known to be critical terrestrial boundary conditions. The two regions adjacent to major impact basins (Hellas and Isidis Planitia) showed radially outward upslope winds driving sand movement, although seasonally reversing wind regimes were also observed. The northern polar dunes yielded the highest known fluxes on the planet, driven by summer katabatic winds modulated by the seasonal CO_2 cap retreat—processes not known to affect terrestrial dunes. In contrast, southern dune fields (<45°S) were less mobile, likely as a result of seasonal frost and ground ice suppressing sand availability. Results suggest that, unlike on Earth, large-scale topographic and thermophysical variabilities play a leading role in driving sand fluxes on Mars.

INTRODUCTION

For most of the history of Mars, eolian processes have been one of the leading factors in landscape evolution, in contrast to Earth and early Mars, where aqueous processes prevailed. Recent orbital studies have revealed that winds frequently transport fine-grained sediments across the surface of Mars today, as evidenced by the mobility of eolian bed forms (dunes and ripples; e.g., Silvestro et al., 2010; Chojnacki et al., 2011, 2017, 2018; Bridges et al., 2011, 2012; Ayoub et al., 2014; Banks et al., 2015, 2018). The degree of contemporary sand mobility has implications for the Martian climate, dust cycle, and landscape evolution. Moreover, spatial variations in bed-form transport parameters relate to external forcing factors (i.e., boundary conditions), some of which may be unique to the red planet.

Terrestrial antecedent conditions, such as near-surface water tables and vegetation, can critically influence local bed-form patterns and mobility. On Mars, factors like crater morphology and local surface roughness can influence sand fluxes (Chojnacki et al., 2017). Large-scale dune construction appears to be extremely limited on Venus (based on orbital radar data; Greeley et al., 1995), whereas bed forms on Titan (a moon of Saturn) cover an estimated ~13% of the surface (from similar data; Le Gall et al., 2012). The numerous extraneous environmental factors on planetary bodies with atmospheres (e.g., transport capacity, sand supply, topography) operate nonlinearly to produce self-organized bed forms that evolve in response to environmental conditions (e.g., Kocurek and Lancaster, 1999; Ewing and Kocurek, 2010). Recognition of these underlying boundary conditions can provide insight into landscape evolution on Mars because eolian processes have played a major role there for most of its history (Armstrong and Leovy, 2005).

The objective of this investigation was to assess the boundary conditions that govern bed-form migration trends on Mars and whether those conditions differ from ones on Earth. Recognizing these factors may also provide predictability for other locations lacking sufficient data for monitoring. This was achieved by quantifying the dynamic activity of bed forms globally and evaluating the regional factors that may play a role.

DATA SETS AND METHODS

To assess bed-form morphology and dynamics, we analyzed images acquired by the High Resolution Imaging Science Experiment (HiRISE) camera on the Mars Reconnaissance Orbiter (0.25–0.5 m/pixel; McEwen et al., 2007; see Table DR1 in the GSA Data Repository[1]). Digital terrain models (1 m/pixel) and orthoimages of dune fields were constructed from HiRISE data using SOCET SET® BAE Systems photogrammetry software (Kirk et al., 2008). Volumetric sand fluxes (q_{crest}) for dunes were obtained using the product of the estimated height and lee crest displacement over the intervening time between acquisition of repeated HiRISE images (2–5 Mars years), measured in units of $m^3\ m^{-1}\ yr^{-1}$ in time units of Earth years. Sand fluxes, migration rates, and heights were collected for 54 dune fields (495 separate dunes). Ripple migration rates were integrated from prior work (Banks et al., 2015, 2018).

To provide regional context for monitoring sites, topographic and thermal properties (albedo and daytime surface temperature) were examined from Mars Orbiter Laser Altimeter data (Smith et al., 2001) and Thermal Emission Spectrometer (on the Mars Global Surveyor) data (Christensen et al., 1992), respectively. See the GSA Data Repository, sections 1 and 2, for additional methodology and boundary condition characterization details, respectively.

RESULTS

Global Results of Bed-Form Transport Parameters

Active eolian bed forms were detected across Mars within craters, canyons, structural fossae, volcanic paterae, polar basins, and extracrater (e.g., plains) terrain (Fig. 1). The average migration rate, typically for barchan or barchanoid dune morphologies, across all sites investigated here was ~0.5 ± 0.4 m/yr (1σ) for dunes ~2–120 m tall. Superposed sub-meter-tall ripples (~40 cm tall, where height estimates were from *in situ* observations; Ewing

[1]GSA Data Repository item 2019150, Figures DR1–DR5, Tables DR1 (list of images), Tables DR2 and DR3 (region summary tables), and Animations DR1–DR8, is available online at http://www.geosociety.org/datarepository/2019/, or on request from editing@geosociety.org.

CITATION: Chojnacki, M., Banks, M.E., Fenton, L.K., and Urso, A.C., 2019, Boundary condition controls on the high-sand-flux regions of Mars: Geology, v. 47, p. 427–430, https://doi.org/10.1130/G45793.1

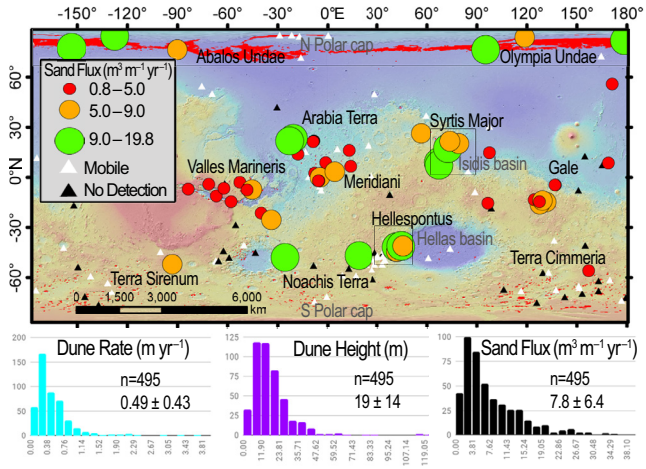

Figure 1. Global trends in bed-form mobility. Top: Map of sand dune crest flux measurements for 54 dune fields (graduated circles with low [red], moderate [orange], and high [green] sand flux values), bed-form mobility detection status (triangles; Banks et al., 2015, 2018), and dune field distributions (red polygons; Hayward et al., 2014). Three high-sand-flux regions of Syrtis Major, Hellespontus Montes, and the north polar erg (Mars) are outlined in black and shown in more detail in Figure 3. Base map is Mars Orbiter Laser Altimeter (MOLA) shaded relief with colorized elevation from +4 (red) to –5 km (blue). Bottom: Histograms of dune metrics with averages ± 1σ.

et al., 2017) showed similar rates (~0.5 m/yr), although examples of faster ripples have often been reported (Bridges et al., 2012). The average q_{crest} for all dune fields ranged between 0.8 and 17.6 $m^3\ m^{-1}\ yr^{-1}$ (Fig. 2), while the highest flux for an individual dune was 35 $m^3\ m^{-1}\ yr^{-1}$ (average q_{crest} = 7.8 ± 6.4 [1σ] $m^3\ m^{-1}\ yr^{-1}$).

Identifications of the Highest-Sand-Flux Regions

Moderate- and high-flux (arbitrarily defined as 5–9 and >9 $m^3\ m^{-1}\ yr^{-1}$, respectively) dune fields clustered (in groups ≥3) in three main regions based on available data: Syrtis Major, Hellespontus Montes, and the north polar erg (Figs. 1 and 2; Fig. DR1). Morphology in these higher-flux locations consistently showed very crisp, distinct slipface brinks as compared with the more rounded lee-side dune faces in some low-flux regions (e.g., Banks et al., 2018). These areas also host larger (migrating) ripples than have been previously reported (Bridges et al., 2011; Banks et al., 2018), with spacing of ~8–18 m and heights of 0.8–2.0 m (e.g., see Animation DR1).

All three regions are located adjacent to prominent topographic transition zones: Syrtis Major west of the Isidis basin, Hellespontus west of the Hellas basin, and the circumpolar erg adjacent to the north polar cap (Figs. 3 and 4). Elevation profiles several hundreds of kilometers in length from basins toward the higher-elevation terrains have 4–7 km in relief, except for the shorter (~2-km-high) but more abrupt north polar cap (Table DR2). These regions show notable absolute albedo variations (10%–25%) and large daytime surface temperature contrasts (3–23 K) along the broad profiles from basin to higher terrain. These factors likely contribute to the high modeled wind speeds for these regions in Ames (NASA Ames Research Center, California, USA) global circulation models (GCMs; Fig. DR2; Bridges et al., 2011; Read et al., 2015). Average sand transport directions are often broadly aligned parallel to regional-scale slopes, which likely correspond to downslope katabatic or upslope anabatic wind regimes. However, migration is not strictly unidirectional, as signs of more complex wind regimes were observed.

DISCUSSION

Global results demonstrate substantial geographic heterogeneity in sand transport rates across the planet and per site. Because boundary conditions dictate many physical aspects of dune morphology and activity, the three regions with remarkably high sand fluxes deserve further consideration.

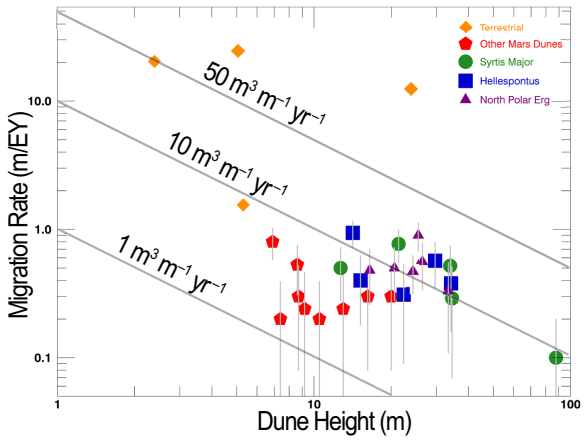

Figure 2. Log-log plot of dune migration rates versus dune heights for select Martian and terrestrial dune fields. Dune rates are averages per site using the longest baseline images available. Migration rate confidence intervals are indicated by vertical error bars (typically ±0.1–0.3 m/yr) and account for orthoimage registration offsets and human error in manual measurements. Syrtis Major, Hellespontus Montes, and north polar erg (Mars) dunes were nearly twice as tall as dunes at other mobile sites (average heights of 28 m versus 15 m). "Terrestrial" group includes dune field data from the Salton Sea (California, USA), Mauritania, Antarctica, and Namibia (Long and Sharp, 1964; Ould Ahmedou et al., 2007; Bourke et al., 2009; Scheidt and Lancaster, 2013). See Table DR1 (see footnote 1) for site information, including "Other Mars Dunes"; see Figure 3 for spatial locations.

Syrtis Major

Dunes across the low-albedo (~0.1) Syrtis Major are found in a variety of geographical contexts (e.g., fossae, paterae, plains, and craters), but their migration vectors appear to be strongly influenced by the 4–5-km-deep Isidis basin to the east (Fig. 3; Table DR2). Westward sand transport at this equatorial latitude is governed by the superposition of the meridional (Hadley cell) overturning circulation and planetary rotation, but this flow is further enhanced by a strong thermal tide and anabatic slope winds driven up and radially outward from the dusty Isidis basin (albedo ~0.23) by daytime solar heating (e.g., Ayoub et al., 2014). Dunes near Jezero crater and deep within Nili Fossae are clearly migrating to the west-northwest (Chojnacki et al., 2018), whereas sand dunes along Nili and Meroe Paterae are translating toward the west-southwest (Fig. 3; see Animations DR1 and DR2 and Table DR1). These latter high-flux dune fields are located immediately downwind of zones of high aerodynamic shear stress (calculated from a mesoscale model) that are enhanced by the local patera topography (Michaels, 2011). Winds in these regions drive sand to abrade surfaces at relatively high rates (~0.1–50 m/m.y.) and contribute to local landscape evolution (Bridges et al., 2012; Chojnacki et al., 2018).

These high sand-flux rates contrast with those of dunes across the cratered plains of Meridiani Planum (Fig. 1), a region at a similar latitude as Syrtis but lacking substantial topography. Meridiani Planum dunes exhibit low sand fluxes except for a few located in the northernmost craters in Arabia Terra adjacent to the global dichotomy (a marked dichotomy in topography, surface age, and crustal thickness between the Martian northern lowland and southern upland) (Chojnacki et al., 2018). Seasonal volatile cycles that negatively affect sand availability in colder regions are not likely to affect bed-form mobility at either of these tropical-latitude locations.

Overall, Syrtis Major boundary conditions include a unidirectional wind regime related to Isidis slope winds that is enhanced by local topography (paterae and fossae) that drive a limited and unconsolidated sand supply at relatively high rates (Fig. 4; Table DR3). Other low-latitude bed forms are mobile (e.g., Gale crater, Meridiani Planum), but at much lower rates (Ewing et al., 2017; Chojnacki et al., 2018).

Hellespontus Montes

Variable-sized crater- and plains-related dune fields are found across the rugged Hellespontus Montes mountain range (Fig. 3). Hellespontus is 10% lower in albedo than Hellas basin to the east (Table DR2). Westward sand transport is most frequently observed here (Animation DR3), but dune

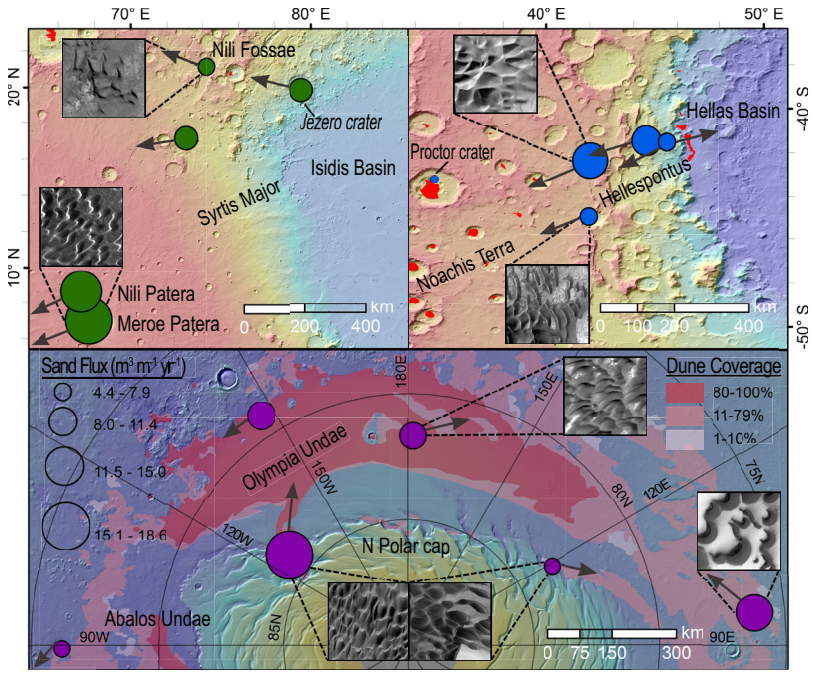

Figure 3. Regions of moderate- and high-sand-flux dune fields (graduated circles with same color scheme as Fig. 2). Legend in bottom map applies to all panels. Average dune migration vectors are represented by black arrows for each dune field. Dune field distributions are shown in red. Inset High Resolution Imaging Science Experiment (HiRISE) images are ~2 km wide. Base maps are Mars Orbiter Laser Altimeter (MOLA) shaded relief with colorized elevation from +4 (red) to –5 km (blue), except for the north polar map, which ranges from –2 to –7 km. Compare with Figure 4.

morphology in other areas suggests at least three formative wind regimes (Fenton, 2005). Bidirectional converging wind systems are evidenced by southwestward- and eastward-migrating dunes and ripples on opposite sides of the same ~5-km-wide dune field (Fig. DR3; Animations DR4 and DR5). This sediment movement appears to be related to topographically enhanced, high-stress surface winds, as modeled by the Ames GCM (e.g., Fig. DR2; Armstrong and Leovy, 2005).

However, the influence of Hellas winds appears to diminish to the southwest across the flatter Noachis Terra plains, where sand fluxes decrease (Banks et al., 2018). The seasonal volatile cycle of CO_2 frost may play a crucial role in the Noachis bed-form sand availability. Ripple migration rates decrease to the southwest of Hellespontus, and migrating dunes are only detected northward of 57°S—these areas show evidence for ground ice and seasonal frost (Fig. DR4; Animation DR6; Fenton and Hayward, 2010; Banks et al., 2018). Carbon dioxide frost also drives gully activity along Noachis crater walls and dune slopes, whereas reports for these are absent in Hellespontus (Fig. DR4; Dundas et al., 2017).

In summary, Hellespontus boundary conditions include a multidirectional wind regime (midlatitude westerlies and Hellas basin slope winds), a moderate sand supply, and rugged terrain that appears to increase local wind shear stress (Fig. 4; Table DR3). These conditions contrast with those in neighboring Noachis Terra, where seasonal volatiles and ground ice negatively impact the sand availability and mobility of local dunes.

North Polar Ergs

The most active dune region on Mars occurs within the expansive north circumpolar ergs of Olympia and Abalos Undae (Fig. 3). A critical boundary condition at these latitudes is the autumn/winter CO_2/H_2O ice accumulation that restricts dune migration for roughly half of the year. Sand becomes ice-cemented while wintertime CO_2 ice buries dunes and then slowly sublimates through the northern spring until bed forms are "frost free" and mobile by summer (Ewing et al., 2010; Hansen et al., 2011). This seasonal CO_2 ice appears to contribute to up to 20% of the local sand movement in the form of large slipface alcoves that develop as the result of overburden along dune crests (Diniega et al., 2017), an apparently unique Martian process. Despite the seasonal sand availability limitation, the region shows extensive eolian activity with widespread ripple, megaripple, and dune migration (Animations DR7 and DR8). Dune q_{crest} values here were ~50% greater than average values for Mars (11.4 versus 7.8 $m^3\ m^{-1}\ yr^{-1}$).

Mesoscale model simulations indicated that spring and summer katabatic winds are driven by the retreat of the seasonal CO_2 and increasingly large thermal and albedo values (15%–25%), along with topographic variations between the ergs and polar cap (Table DR2; Smith and Spiga, 2018). Peak modeled winds and observed sand fluxes occur at cap boundary locations. Sand patches emanate from the Planum Boreum deposit cliffs, forming protodunes and barchans, and coalescing into larger barchanoidal dunes downwind (Animation DR8; Fig. DR5). Numerous 20–30-m-tall dunes translate at relatively high rates (~1 m/yr) tangentially away from the polar scarp and are then steered zonally by Coriolis-force–directed winds (Ewing et al., 2010); more moderate sand fluxes occur along distal locations of the southern erg margin where other wind regimes are a factor.

Like the north polar ergs, south polar dune fields also experience ground and seasonal ice, but they show limited bed-form movement (Fig. 1; Banks et al., 2018). This contrast in sand mobility is attributed to the greater relief and katabatic winds of the northern cap, along with the longer and colder winters (longer duration of frost coverage) and higher regional elevation (lower surface

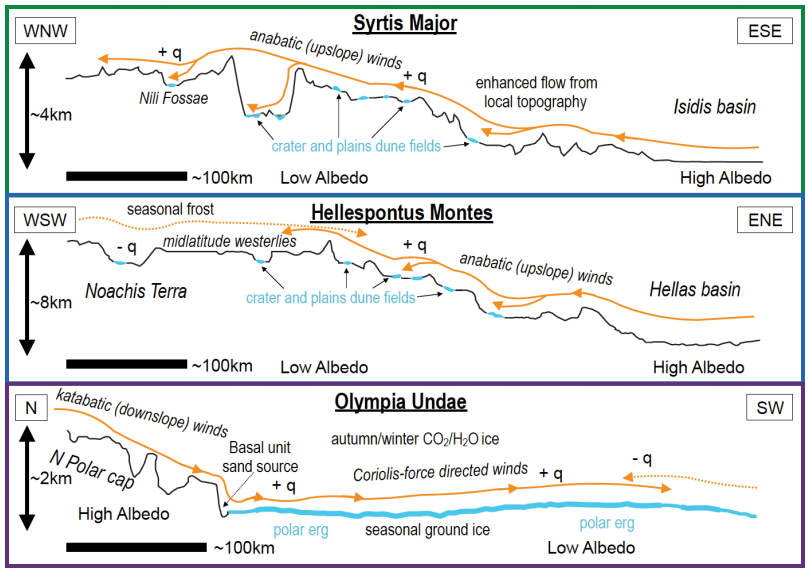

Figure 4. Schematic representation of regional boundary condition elements. Mars Orbiter Laser Altimeter (MOLA) topographic profiles are shown, where thicker blue lines indicate locations of dune fields and increased sediment supply. Primary (orange solid lines) and secondary (orange dashed lines) wind regimes and locations of relatively high (+*q*) and low (–*q*) sand fluxes are shown. Compare with Figure 3, and see text and Tables DR2 and DR3 (see footnote 1) for details.

pressure) in south polar areas (e.g., Banks et al., 2018). Site elevation, and its indirect effects on saltation threshold with pressure, is another global control that should be considered in assessing sand mobility (Armstrong and Leovy, 2005).

Overall, external factors for the north polar ergs include a high sand supply that has restricted availability during the colder seasons by ice, but also a complex wind regime where strong summertime katabatic winds contribute to the highest fluxes observed on Mars (Fig. 4; Table DR3).

CONCLUSIONS

We quantified bed-form sand fluxes across Mars, finding that the largest fluxes are driven by boundary conditions distinct from those on Earth. The locations of Syrtis Major, Hellespontus Montes, and the north polar erg are all near prominent topographic boundaries (e.g., impact basins, the polar cap), which also have strong thermal gradients that likely contribute to seasonal winds and, in turn, high sand mobility. Katabatic and anabatic wind regimes may constructively combine with flows driven or steered by synoptic-scale forcing (e.g., the thermal tide, tropical meridional overturning, the Coriolis force) to drive sand along regional-scale slopes. Seasonal volatiles (CO_2/H_2O frost) and ground ice at higher latitudes play a critical role in inhibiting or contributing to sand availability or mobility. The largest sand fluxes occur along the north polar cap where seasonally retreating CO_2 and a large thermal contrast drive geomorphically effective winds. Although some high-flux wind regimes are unidirectional, other sites show that bidirectional winds drive convergent dune migration patterns. Moreover, our finding of enhanced sand fluxes in the vicinity of large-scale topographic and thermophysical variability is consistent with previous work demonstrating that these factors play a more critical role for wind flow on Mars than on Earth (e.g., Read et al., 2015).

ACKNOWLEDGMENTS

We appreciate the constructive input from reviewers Ryan C. Ewing, Jean-Philippe Avouac, and Mackenzie Day, whose input greatly improved this manuscript. This research was supported in part by NASA Mars Data Analysis Program grants NNH14ZDA001N (Chojnacki, Urso) and NNX14AO96G (Banks), and the HiRISE/Mars Reconnaissance Orbiter mission. We would like to thank HiRISE operations students and staff for assistance with targeting and digital terrain model production.

REFERENCES CITED

Armstrong, J.C., and Leovy, C.B., 2005, Long term wind erosion on Mars: Icarus, v. 176, p. 57–74, https://doi.org/10.1016/j.icarus.2005.01.005.

Ayoub, F., Avouac, J.-P., Newman, C.E., Richardson, M.I., Lucas, A., Leprince, S., and Bridges, N.T., 2014, Threshold for sand mobility on Mars calibrated from seasonal variations of sand flux: Nature Communications, v. 5, p. 5096, https://doi.org/10.1038/ncomms6096.

Banks, M.E., Geissler, P.E., Bridges, N.T., Russell, P., Silvestro, S., Chojnacki, M., Zimbelman, J.R., and Delamere, W.A., 2015, Emerging global trends in aeolian bedform mobility on Mars, *in* Fourth Annual International Planetary Dunes Workshop, 19–22 May, Boise Idaho: Lunar and Planetary Institute, abstract 8036, https://www.hou.usra.edu/meetings/dunes2015/pdf/8036.pdf.

Banks, M.E., Fenton, L.K., Bridges, N.T., Geissler, P.E., Chojnacki, M., Runyon, K.D., Silvestro, S., and Zimbelman, J.R., 2018, Patterns in mobility and modification of middle- and high-latitude Southern Hemisphere dunes on Mars: Journal of Geophysical Research–Planets, v. 123, p. 3205–3219, https://doi.org/10.1029/2018JE005747.

Bourke, M.C., Ewing, R.C., Finnegan, D., and McGowan, H.A., 2009, Sand dune movement in the Victoria Valley, Antarctica: Geomorphology, v. 109, p. 148–160, https://doi.org/10.1016/j.geomorph.2009.02.028.

Bridges, N.T., et al., 2011, Planet-wide sand motion on Mars: Geology, v. 40, p. 31–34, https://doi.org/10.1130/G32373.1.

Bridges, N.T., Ayoub, F., Avouac, J.-P., Leprince, S., Lucas, A., and Mattson, S., 2012, Earth-like sand fluxes on Mars: Nature, v. 485, p. 339–342, https://doi.org/10.1038/nature11022.

Chojnacki, M., Burr, D.M., Moersch, J.E., and Michaels, T.I., 2011, Orbital observations of contemporary dune activity in Endeavor crater, Meridiani Planum, Mars: Journal of Geophysical Research, v. 116, E00F19, https://doi.org/10.1029/2010JE003675.

Chojnacki, M., Urso, A.C., Fenton, L.K., and Michaels, T.I., 2017, Aeolian dune sediment flux heterogeneity in Meridiani Planum, Mars: Aeolian Research, v. 26, p. 73–88, https://doi.org/10.1016/j.aeolia.2016.07.004.

Chojnacki, M., Banks, M., and Urso, A., 2018, Wind-driven erosion and exposure potential at Mars 2020 rover candidate-landing sites: Journal of Geophysical Research–Planets, v. 123, p. 468–488, https://doi.org/10.1002/2017JE005460.

Christensen, P.R., et al., 1992, Thermal Emission Spectrometer Experiment: Mars Observer Mission: Journal of Geophysical Research, v. 97, p. 7719, https://doi.org/10.1029/92JE00453.

Diniega, S., Hansen, C.J., Allen, A., Grigsby, N., Li, Z., Perez, T., and Chojnacki, M., 2017, Dune-slope activity due to frost and wind throughout the north polar erg, Mars, *in* Conway, S.J., et al., eds., Martian Gullies and their Earth Analogues: Geological Society of London Special Publications, v. 467, https://doi.org/10.1144/SP467.6.

Dundas, C.M., McEwen, A.S., Diniega, S., Hansen, C.J., Byrne, S., and McElwaine, J.N., 2017, The formation of gullies on Mars today, in Conway, S.J., et al., eds., Martian Gullies and their Earth Analogues: Geological Society of London Special Publications, v. 467, p. 67–94, https://doi.org/10.1144/SP467.5.

Ewing, R.C., and Kocurek, G., 2010, Aeolian dune-field pattern boundary conditions: Geomorphology, v. 114, p. 175–187, https://doi.org/10.1016/j.geomorph.2009.06.015.

Ewing, R.C., Peyret, A.-P.B., Kocurek, G., and Bourke, M., 2010, Dune field pattern formation and recent transporting winds in the Olympia Undae dune field, north polar region of Mars: Journal of Geophysical Research–Planets, v. 115, E08005, https://doi.org/10.1029/2009JE003526.

Ewing, R.C., et al., 2017, Sedimentary processes of the Bagnold Dunes: Implications for the eolian rock record of Mars: Journal of Geophysical Research–Planets, v. 122, p. 2544–2573, https://doi.org/10.1002/2017JE005324.

Fenton, L.K., 2005, Potential sand sources for the dune fields in Noachis Terra, Mars: Journal of Geophysical Research, v. 110, E11004, https://doi.org/10.1029/2005JE002436.

Fenton, L.K., and Hayward, R.K., 2010, Southern high latitude dune fields on Mars: Morphology, aeolian inactivity, and climate change: Geomorphology, v. 121, p. 98–121, https://doi.org/10.1016/j.geomorph.2009.11.006.

Greeley, R., Bender, K., Thomas, P.E., Schubert, G., Limonadi, D., and Weitz, C.M., 1995, Wind-related features and processes on Venus: Summary of *Magellan* results: Icarus, v. 115, p. 399–420, https://doi.org/10.1006/icar.1995.1107.

Hansen, C.J., et al., 2011, Seasonal erosion and restoration of Mars' northern polar dunes: Science, v. 331, p. 575–578, https://doi.org/10.1126/science.1197636.

Hayward, R.K., Fenton, L.K., and Titus, T.N., 2014, Global Digital Dune Database (MGD3): Global dune distribution and wind pattern observations: Icarus, v. 230, p. 38–46, https://doi.org/10.1016/j.icarus.2013.04.011.

Kirk, R.L., et al., 2008, Ultrahigh resolution topographic mapping of Mars with MRO HiRISE stereo images: Meter-scale slopes of candidate *Phoenix* landing sites: Journal of Geophysical Research, v. 113, E00A24, https://doi.org/10.1029/2007JE003000.

Kocurek, G., and Lancaster, N., 1999, Aeolian system sediment state: Theory and Mojave Desert Kelso dune field example: Sedimentology, v. 46, p. 505–515, https://doi.org/10.1046/j.1365-3091.1999.00227.x.

Le Gall, A., Hayes, A.G., Ewing, R., Janssen, M.A., Radebaugh, J., Savage, C., and Encrenaz, P., 2012, Latitudinal and altitudinal controls of Titan's dune field morphometry: Icarus, v. 217, p. 231–242, https://doi.org/10.1016/j.icarus.2011.10.024.

Long, J.T., and Sharp, R.P., 1964, Barchan-dune movement in Imperial Valley, California: Geological Society of America Bulletin, v. 75, p. 149–156, https://doi.org/10.1130/0016-7606(1964)75[149:BMIIVC]2.0.CO;2.

McEwen, A.S., et al., 2007, Reconnaissance Orbiter's High Resolution Imaging Science Experiment (HiRISE): Journal of Geophysical Research, v. 112, E05S02, https://doi.org/10.1029/2005JE002605.

Michaels, T.I., 2011, Aeolian phenomena at Nili and Meroe Paterae, *in* Lunar and Planetary Science Conference XLII, 7–11 March, The Woodlands, Texas: Lunar and Planetary Institute, abstract 2697, https://www.lpi.usra.edu/meetings/lpsc2011/pdf/2697.pdf.

Ould Ahmedou, D., Ould Mahfoudh, A., Dupont, P., Ould El Moctar, A., Valance, A., and Rasmussen, K.R., 2007, Barchan dune mobility in Mauritania related to dune and interdune sand fluxes: Journal of Geophysical Research–Earth Surface, v. 112, F02016, https://doi.org/10.1029/2006JF000500.

Read, P.L., Lewis, S.R., and Mulholland, D.P., 2015, The physics of Martian weather and climate: A review: Reports on Progress in Physics, v. 78, p. 125901, https://doi.org/10.1088/0034-4885/78/12/125901.

Scheidt, S.P., and Lancaster, N., 2013, The application of COSI-Corr to determine dune system dynamics in the southern Namib Desert using ASTER data: Earth Surface Processes and Landforms, v. 38, p. 1004–1019, https://doi.org/10.1002/esp.3383.

Silvestro, S., Fenton, L.K., Vaz, D.A., Bridges, N.T., and Ori, G.G., 2010, Ripple migration and dune activity on Mars: Evidence for dynamic wind processes: Geophysical Research Letters, v. 37, L20203, https://doi.org/10.1029/2010GL044743.

Smith, D.E., et al., 2001, Orbiter Laser Altimeter: Experiment summary after the first year of global mapping of Mars: Journal of Geophysical Research, v. 106, p. 23689–23722, https://doi.org/10.1029/2000JE001364.

Smith, I.B., and Spiga, A., 2018, Seasonal variability in winds in the north polar region of Mars: Icarus, v. 308, p. 188–196, https://doi.org/10.1016/j.icarus.2017.10.005.

Printed in USA